The authors appreciate the points listed above by the PAC. Each will be explained below:

1. The minimum intensity that ensures the feasibility of the experiment is 2x10^5 pps/μC at UC_x resulting in 1.6x10^4 pps at the MINIBALL target position (Case1)

T-REX particle array has an acceptance of 60% for the particle detection (confirmed from the simulations). With a 1.2 mg/cm2 target thickness and 1.6×10^4 pps of a beam intensity, an absolute photo-peak efficiency of 6% at 1 MeV for MINIBALL, and an average cross section of 20 mb for the $2d_{5/2}$ and 28 mb for the $3s_{1/2}$ states:

- Over 600 particle-γ rays and ~40 particle-γγ coincidence events on average for the $2d_{5/2}$ states from 2^+ to 7^+
- Around 900 particle-γ rays and 50 particle-γγ coincidence events for each $3s_{1/2}$ state (i.e. 4^+ and 5^+) are expected after 7 days of beam time.

2. The results of the simulations are given below. Note that simulations have been performed not only for the intensity mentioned above but also for the intensity suggested by the TAC, i.e. 5x10^4 pps/μC at UC_x resulting in 4x10^3 pps at the MINIBALL target position for comparison.

Case1: 16000 pps at MINIBALL, Target thickness: 1.2 mg/cm^2 , E(^{79}Zn)=5 MeV/nuc

Case2: 4000 pps at MINIBAL, Target thickness: 2mg/cm^2 , E(^{79}Zn)=5 MeV/nuc

Short explanations on the simulations: The simulations have been performed using nptool [1]. The level scheme, the differential cross sections obtained using the code FRESCO as well as the excitation energies given in Figure 1 are used as inputs in the calculations. The results shown in Figures 2, 3, and 4 are obtained for the 5^+ (l=2) state at 3.7 MeV and 4^+ (l=0) state at 3.9 MeV. Three transitions are decaying from each of the these states, i.e. 526-880-1721 keV and 726-1080-1921 keV, respectively. Their branching ratios are assumed to be equal and ~33% for each.

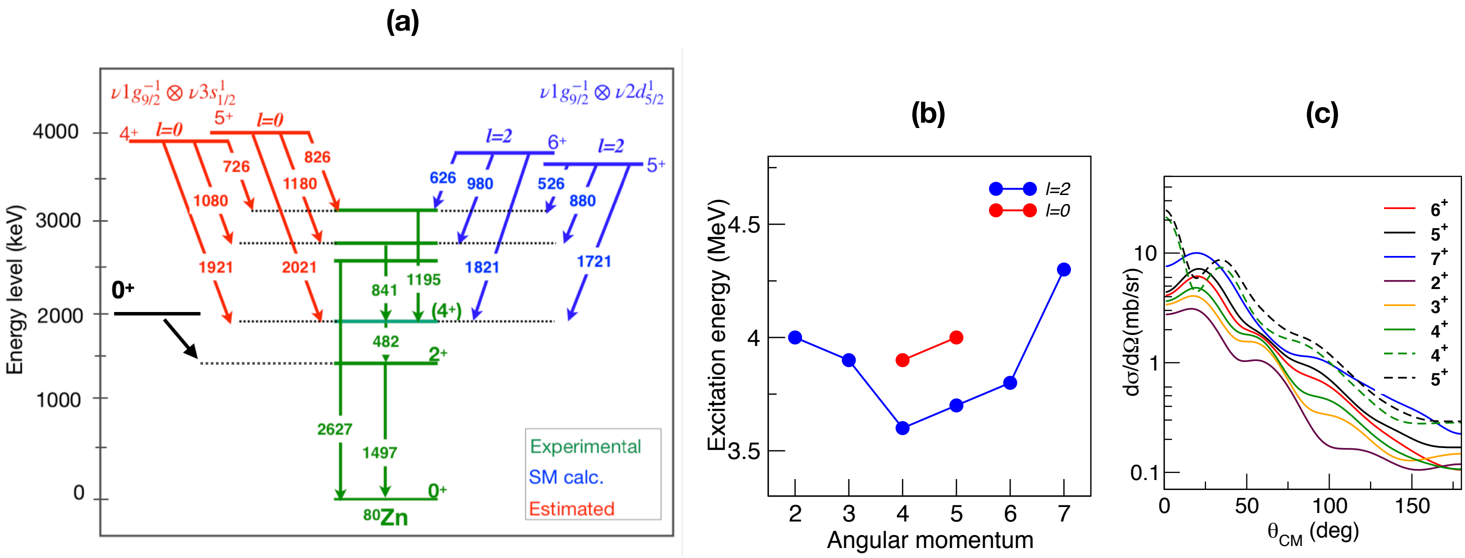

Figure 1: (a) Level scheme of ^{80}Zn. (b) Excitation energies are expected to form a parabola as a result of neutron $(g_{9/2})^{-1}$ $(d_{5/2})$ interaction. Similar parabolas are obtained for ^{90}Zr and ^{88}Sr, the other two members of the N=50 isotonic chain. (c) Differential cross sections for the $2d_{5/2}$ states (solid lines) and for the two $3s_{1/2}$ states (dashed lines).

The Figure 2a shows the proton energy as a function of scattering angle in the laboratory frame. The simulations include the geometry of the TREX array and result in 60% of the acceptance. The gamma-ray spectrum shown in Figure 2b is obtained by gated on the proton distribution in Figure 2a. Gamma transitions are following the colour code in the level scheme given in Figure 1a. Transitions reflect the intensity expected after 7 days of beam time after considering 6% of the efficiency at 1 MeV for MINIBALL.

3. Strategy to determine spin and parity:

Case1:

(i) **Level scheme reconstruction** can be done via combination of p-γγ coincidences and the corresponding incoming excitation energies: First particle gated γγ coincidence data is used to check transitions in coincidence and the order of these transitions is determined by obtaining the γ gated excitation distribution for each gamma ray within the cascade. This then allows one to reconstruct the excitation energies via gamma-cascades. The procedure was applied in Ref. [2]. Such gates are shown in Figure 2c and d. Gates are chosen to be 526 keV and 726 keV decaying from the states 3.7 MeV (l=2) and 3.9 MeV (l=0), respectively. Both FWHM and the centroid of the resulting excitation energy distributions are given in the figures. Figures show that the gamma gated excitation energies are resolved within 200 keV.

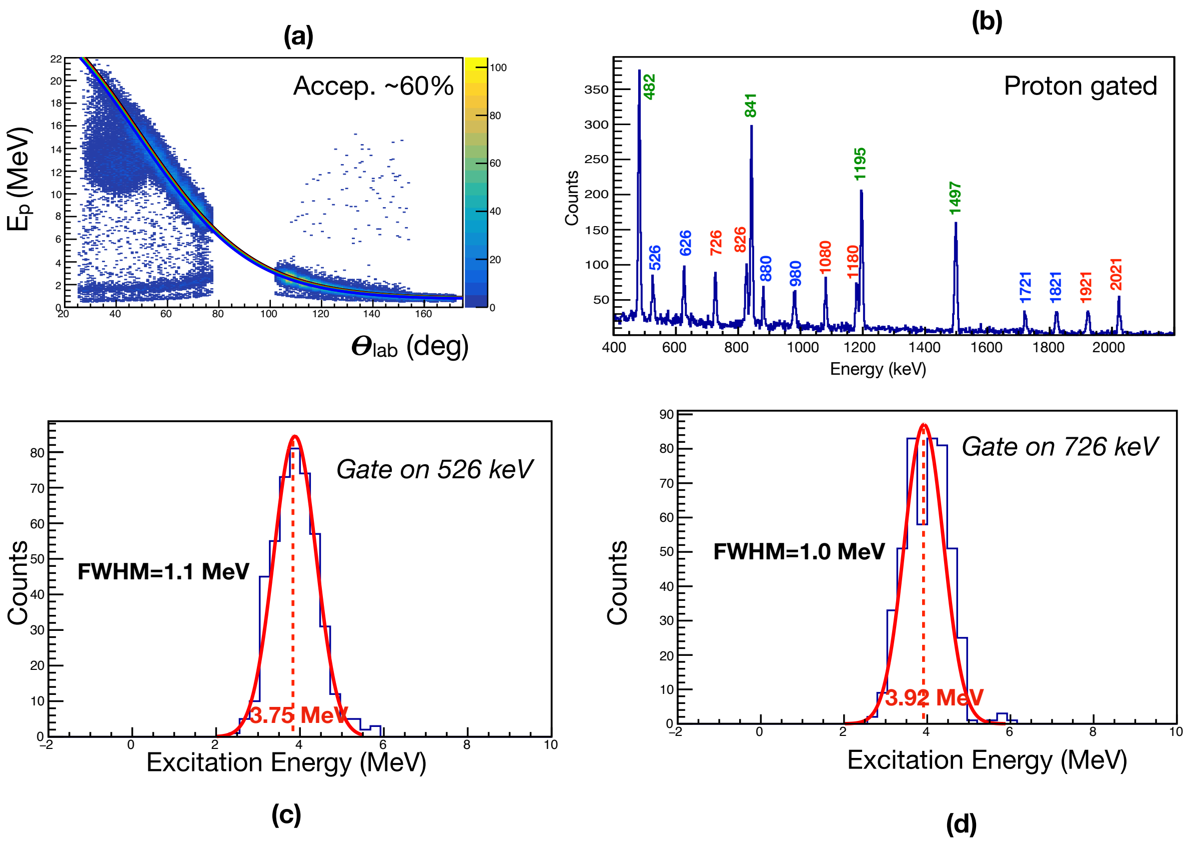

Figure 2: Results of the Simulations performed for Case1: 16000 pps beam intensity on a 1.2 mg/cm^2 target at an energy of 5 MeV/nuc

(ii) **Proton angular distributions** are obtained from the p-γ events. Figure 4a shows the proton angular distribution gated on the gamma-rays decaying from the state of interest. The sum of the γ gates at 526, 880, and 1721 keV is used for the 3.7-MeV state and the gates of 726, 1080, and 1921 keV are summed for the 3.9-MeV state. The comparison of these distributions to the DWBA estimations indicates that the l = 2 and l = 0 angular momentum transfers as well as the spin of the expected states can be identified once the proton scattering distributions are selected via proper γ-ray tagging.

(iii) **Gamma-ray angular distributions** will be complimentary to identify the spins of the populated states from 2^+ to 7^+ (l=2) and from 4^+ to 5^+ (l=0). Catford et al. showed a novel technique applying gamma-ray angular distributions to a (d,pγ) transfer reaction performed at

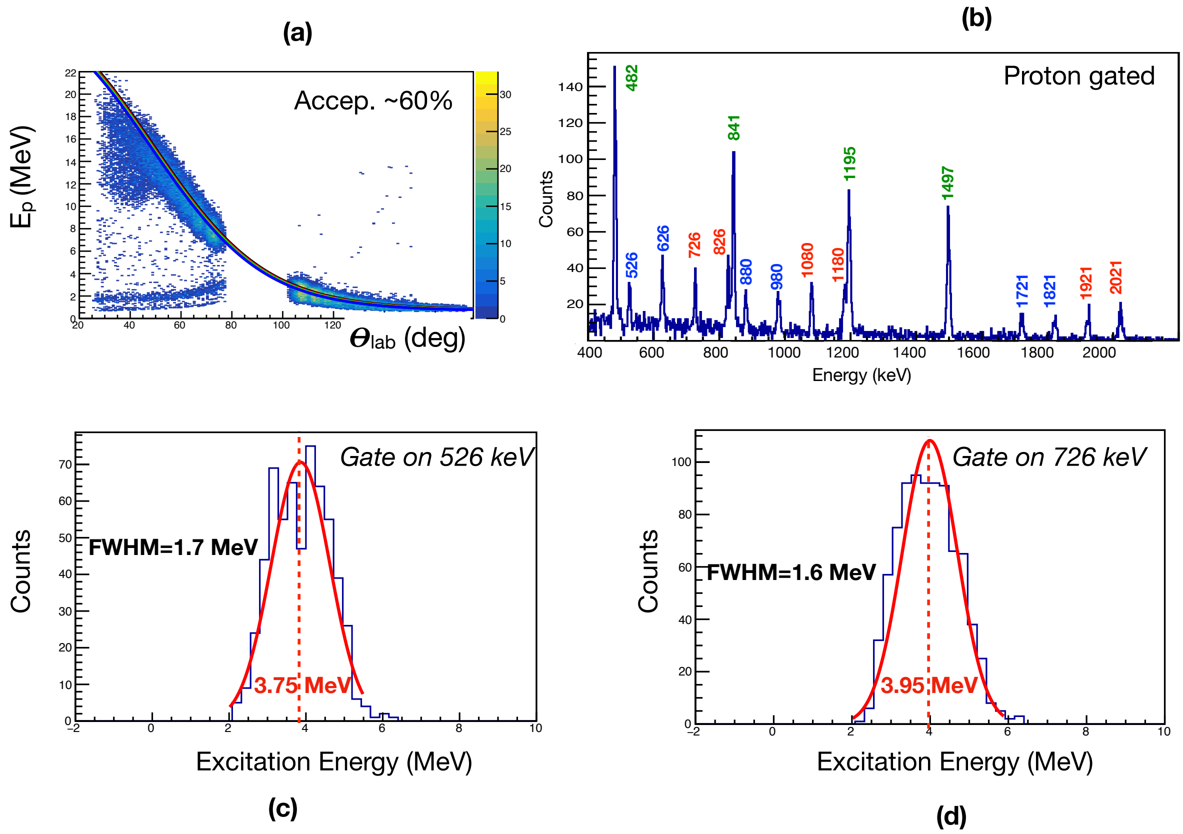

Figure 3: Results of the Simulations performed for Case1: 4000 pps beam intensity on a 2 mg/cm^2 target at an energy of 5 MeV/nuc

TRIUMF. The SHARC-TIGRESS arrays were used in the experiment [3]. The technique showed that γ-ray angular distributions depend on the detection angle of the scattered proton and analysis was performed for nine strong transitions obtained in the reaction. However, due to the weak population of gamma transitions for more exotic channels, the paper also discussed the possibility of obtaining γ-ray angular distributions averaged over all possible scattering angles of protons. Such an analysis will be applied in the present case by considering possible scattering angles of protons from 25 to 70 and from 105 to 165 degrees in laboratory frame and by considering possible ϑ Polar angles of MINIBALL crystals with respect to the beam direction. Polar angles of MINIBALL are covering from ~60 to ~130 degrees in experiments combined to particle detectors at ISOLDE.

Finally obtained results will be compared to shell model (SM) calculations. Such calculations were performed a decade ago only for the 5^+ and 6^+ (l=2) states with limited computing power [4,5]. The present experiment will provide data for SM, which were not feasible 10 years ago. Conversely, the calculation can help to guide building the level scheme which is in particular important for Case2 with lower statistics.

In conclusion, the steps described above are achievable with the requested beam intensity of 16000 pps. This is the minimum intensity required in order to achieve the goals of the experiment.

Case2:

In Case2, poor statistics will make the proposed analysis steps above rather difficult. γγ coincidence data will not be sufficient to disentangle the level scheme but p-γ data will be sufficient to perform useful p-γ analysis and to get information about excitation energies.

The incoming excitation energies would be still used to build the level scheme by gating on individual gamma-rays. The examples are shown in Figure 3c and d. Gates are chosen to be 526 keV and 726 keV decaying from the states 3.7 MeV (l=2) and 3.9 MeV (l=0), respectively. Both FWHM and the centroid of the resulting excitation energy distributions are given in the figures. Figures show that the gamma gated excitation energies are still resolvable within 200 keV.

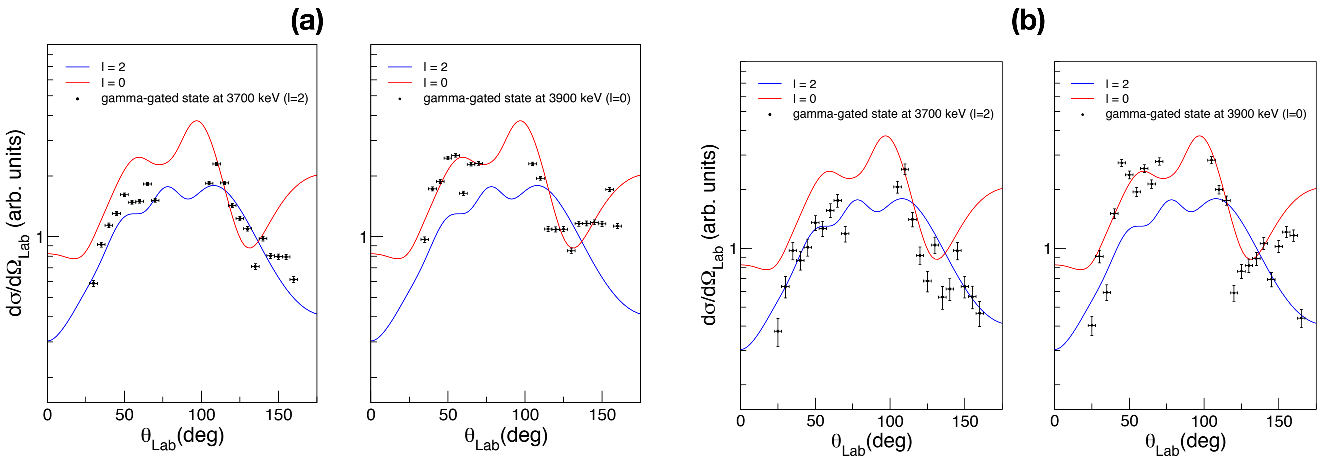

Figure 4: Simulated gamma-gated differential cross sections for the states at 3.7 (l = 2) and 3.9 MeV (l = 0). The DWBA calculations for l = 2 and l = 0 are included for comparison in both cases. (a) Case1 (b) Case2.

Figure 4b shows that different behaviour of the gamma-gated differential cross sections for the states from the l=0 and l=2 transfers. This information will be helpful for the identification of the states from different angular transfer.

We also have to keep in mind that excitation energies are expected to form a parabola as a result of neutron $(g_{9/2})^{-1}$ $(d_{5/2})$ interaction (See Figure 1b). In addition, the excitation energies of the 4^{+} and 5^{+} states from the l=0 transfer $((g_{9/2})^{-1}$ $(s_{1/2}))$ are expected to appear higher in energy compared to the 4^{+} and 5^{+} energies from the l=2 transfer.

For the identification of the states from the l=2 transfer, DWBA calculations show a decreasing trend from 7^{+}, being the state with the highest cross section in Figure 1c, which can be helpful to assign spins from the p-γ analysis.

In conclusion, γγ data is not feasible in Case2, but we will still obtain useful p-γ data. Simulations indicate poorer resolution and analysis will be more difficult since more background is expected in a real situation. Nevertheless, the results for Case2 suggest that even lower beam intensity will give valuable results. This also means that if we start at 16000 pps (in Case1) and the beam intensity decreases somewhat over time, the main goals will still be achievable.

4. With regards to the $1/2^+$ isomer component of the beam, in the work of Yang et al. [6], the halflife of the isomeric state could be given with a lower limit of 200 ms. If we assume the halflife of the isomeric state to be 200 ms, it is around 4 times shorter than the halflife of the ground state (746 ms). This will certainly give a less population of the (2p-2h) state compared to the I=2 and I=0 1p-1h states in ^{80}Zn.

As there is no information on the isomeric ratio, it is difficult to give a quantitative estimate. The isomeric ratios for the odd-mass Zn isotopes depend strongly on the half-lives of gs and isomer [6]. As the $T_{1/2}$ for the gs and isomeric state are comparable to the case of ^{79}Zn, we expect a relatively weak isomeric component in the beam. We consider the identification as a bonus goal of the experiment, which seems achievable for isomeric ratios above a few percent. In this case, the energy of the state was determined to be 1.1 MeV (1p-2h) from Orlandi et al. [7], a possible (2p-2h) should be expected to lie around twice of the (1p-2h) state due to one more p-h interaction. This translates into an energy around 2 MeV which could possibly decay to the 2+ state at 1497 keV (The level is indicated in black colour in Figure 1a). A transition around 400 keV can be a sign of such state and it should not be in coincidence with the 482 keV transition from 4^+ to 2^+ state but with the 2^+ to 0^+ transition at 1497 keV. In case of Case1, the higher beam intensity could provide a unique gamma-ray angular distribution thus the multipolarity of this state.

If the rates cannot be maintained during the whole beamtime in Case1, we can replace the 1.2 mg/cm^2 target with 2mg/cm^2 thick target.

References:

[1] A Matta et al. J. Phys. G: Nucl. Part. Phys. 43 045113 (2016).

[2] J. Diriken et al., Phys. Rev. C 91, 054321 (2015).

[3] W.N. Catford et al., Acta Physica Polonica B46, 527 (2015).

[4] K. Sieja and F. Nowacki, Phys. Rev. C 85 051301(R) (2012).

[5] E. Sahin et al., Nucl. Phys. A 893, 1-12 (2012).

[6] X. F. Yang et al., PRL 116, 182502 (2016).

[7] R.Orlandi et al., Phys. Letts. B 740, 298 (2015).